BCCS
TECHNICAL REPORT SERIES

A study of flow over a backward-facing step and flow over a depression, using the 2D version of Bergen Ocean Model

**Kristin Rygg, Guttorm Alendal,
Peter M. Haugan**

REPORT No. 26 **January 12, 2010**

Deliverance to the Research Council of Norway through the project "Understanding coral distribution and conditions for growth in Norwegian Waters" (Cordino). Contract number 146526/420

UNI Research
the University of Bergen research company

BERGEN, NORWAY

BCCS Technical Report Series is available at http://www.bccs.uni.no/publications/

Requests for paper copies of this report can be sent to:

Bergen Center for Computational Science, Høyteknologisenteret,
Thormøhlensgate 55, N-5008 Bergen, Norway

Abstract

The occurrence of Lophelia pertusa has previously been found correlated with hills and depressions at the bottom of the sea. In order to search for flow patterns related to continuous food transport to the deep-water corals, we have studied flow over a backward-facing step and flow over a depression. The model results correspond with previous published results and gives a basis for justifying the use of Bergen Ocean Model for future coral reef studies. Additionally the study indicates that the recirculation zone is a zone probably not suitable for living corals.

1 Introduction

Lophelia pertusa, is a common benthic habitat in Norwegian waters, and large efforts have been made in order to map the locations of the coral reefs. It has been estimated that the biologic diversity is approximately three times higher in the vicinity of coral reefs compared to elsewhere, and the reefs are therefore known as good fishing places [Fosså et al., 2002].

Though coral reefs have been the focus of attention for some time, there is still a lack of knowledge related to the ecological importance of cold water coral reefs, food supply and important factors for growth [Freiwald et al., 2004]. In the Træna reef area in Lofoten, there have been observed coral reefs that are elongated with the main current, leading to the hypothesis that stable current conditions causing a constant transport of food, might be important for coral growth.

Previous studies have found that coral reefs are often situated on topographic heights or breaks of the seabed [Lindberg et al., 2007]. The hypothesis is that these topographic features either lead to higher local velocities or create current patterns which lead to a constant food supply, maybe due to formation of eddies and retention of particles [Mortensen et al., 2001]. Pockmarks with a vertical extent of 50-100 meters and a depth of 3-10 meters are common on parts of the shelf [Hovland and Judd, 1988], so are also plough marks made from ice berg scouring [Lien, 1983]. There are indications that corals tend to settle close to such features [Freiwald et al., 1999].

Previously, flow over a bell shaped reef have been studied [Thiem et al., 2008]. In this report we will focus on flow over depressions. As a preparation to future 3D studies of flow over pockmarks or plough marks, we have performed studies of flow over a backward-facing step and flow over a long depression using the 2D version of Bergen Ocean Model.

Results from simulations of flow over a backward facing step are compared with published observations in order to test the model setup including resolution and choice of vertical eddy viscosity.

2 Numerical approach

The simulations are done using the 2D mpi version of the σ-coordinate model Bergen Ocean Model, BOM [Berntsen, 2004]. The governing equations are the Reynolds averaged momentum equations using the Boussinesq approximation. Hence the density changes is only included in the gravity term. Additionally the effect of rotation is neglected, leading to the following momentum equations,

$$\frac{\partial U}{\partial t} + \frac{\partial U^2}{\partial x} + \frac{\partial UW}{\partial z} = -\frac{1}{\rho_0}\frac{\partial P}{\partial x} + \frac{\partial}{\partial x}(A_M \frac{\partial U}{\partial x}) + \frac{\partial}{\partial z}(K_M \frac{\partial U}{\partial z}) \, , \tag{1}$$

$$\frac{\partial W}{\partial t} + \frac{\partial UW}{\partial x} + \frac{\partial W^2}{\partial z} = -\frac{1}{\rho_0}\frac{\partial P}{\partial z} - \frac{\rho g}{\rho_0} + \frac{\partial}{\partial x}(A_M \frac{\partial W}{\partial x}) + \frac{\partial}{\partial z}(K_M \frac{\partial W}{\partial z}) \, . \tag{2}$$

We also use the equation of continuity of an incompressible fluid,

$$\frac{\partial U}{\partial x} + \frac{\partial W}{\partial z} = 0 \, . \tag{3}$$

In Equation (1)-(3), $U(x, z, t)$ represents the horizontal velocity, $W(x, z, t)$ the vertical velocity, $P(x, z, t)$ the pressure, $\rho(x, z, t)$ the density, ρ_0 a reference density, g the constant of gravity, A_M, the horizontal eddy viscosity and K_M the vertical eddy viscosity.

For the density, ρ, a conservation equation is used,

$$\frac{\partial \rho}{\partial t} + \frac{\partial U\rho}{\partial x} + \frac{\partial W\rho}{\partial z} = \frac{\partial}{\partial x}(A_H \frac{\partial \rho}{\partial x}) + \frac{\partial}{\partial z}(K_H \frac{\partial \rho}{\partial z}) \, , \tag{4}$$

where A_H represents horizontal eddy diffusivity, and K_H vertical eddy diffusivity. In order to close the system, values of the eddy viscosities and diffusivities must be chosen. In the horizontal the eddy viscosities, A_M are set to 10^{-2} m ^{2} s^{-1} in order to remove numerical noise from the simulations. The horizontal eddy diffusivities, A_H are set to 0. K_M is set equal to K_H, and values between 10^{-2} m^2 s^{-1} to 10 $^{-6}$ m^2 s^{-1} are used.

The pressure at a depth z is expressed by,

$$P(x,z,t) = g\rho_0\eta(x,t) + g\int_z^0 \rho(x,z',t)dz' + P_{NH}(x,z,t) \ , \tag{5}$$

[Berntsen, 2004] where the first term on the right hand side represents pressure due to the surface elevation, η, the second term the internal pressure, and the last term is a non-hydrostatic correction term due to internal movements in the fluid [Marshall et al., 1997a]. When the vertical length scale becomes of the same magnitude as the horizontal length scale the hydrostatic assumption breaks down. According to Marshall et al. [1997b] the hydrostatic assumption begins to break down at a horizontal grid size between 1 and 10 kilometers, or if the vertical velocity is comparable with the horizontal in magnitude. In the simulations in this report, the grid size are from 12 meters and downward, and non-hydrostatic effects are hence important. In BOM the non-hydrostatic pressure is solved using a successive over-relaxation (SOR) method. The iterations continues until the relative error measured in the 2-norm for the vector is less than 10^{-4} [Berntsen et al., 2006] or the number of iterations have reached a maximum number of 50.

At the bottom a quadratic drag is used as specified by [Berntsen, 2004],

$$\vec{\tau}_x = \rho_0 C_D |U_b| U_b \ , \tag{6}$$

where U_b represents the velocity in the lowest grid cell above the bottom, and the drag coefficient, C_D has been chosen set to 5.2·10^{-3} in all simulations.

2.1 Particle tracking

Passive tracers that advect with the currents are included in one simulation. The location of a particle, x_p at the time step, n, is described by

$$\vec{x}_p^{n+1} = \vec{x}_p^n + \Delta t \vec{u}^n \ , \tag{7}$$

where Δt is the time step and $\vec{u}^n$ the velocity of the water at the tracer location at the time step n. A random step for the particles are implemented both in the horizontal and the vertical,

$$\vec{x}_p^{n+1} = \vec{x}_p^{n+1} + r \cdot \Delta t \vec{u}_{std}^n \ , \tag{8}$$

where r is a random number between zero and one, and $\vec{u}_{std}^n$ represents the standard deviation of the velocity components at the time step n. A particle that is within 0.25 meters distance from the bottom is considered eaten by the coral and taken out of the simulation. The location where it is taken out is identified and stored. Periodic boundary conditions are used for the particles.

2.2 Open boundaries

The open boundaries are set using the Flow Relaxation Scheme (FRS) described by Martinsen and Engedahl [1987]. The relaxation zone consists of the 7 outer horizontal cells on the boundaries. The relaxation scheme updates the variables η, U, and ρ in the FRS-zones using the equations [Martinsen and Engedahl, 1987],

$$\tilde{\phi} = \alpha\hat{\gamma} + (1-\alpha)\tilde{\gamma} \ . \tag{9}$$

Here ϕ represents η, U, and ρ, and a variable marked by tilde represents the time-integrated unrelaxed value from the ocean model. A variable with hat represents the prescribed specified value at the boundary. The relaxation parameter, α varies between 0 and 1 within the FRS-zone, set equal to 1 at the outer edge of the FRS-zone and decreases gradually to 0 at the internal boundary of the FRS-zone [Martinsen and Engedahl, 1987].

3 Backward facing rounded step

Flow over a backward-facing step is a well-known test case for numerical methods. It is popular due to its simplicity combined with its complex flow characteristics. For flow over a sharp backward-facing step the separation line is at the edge of the step (Neumann and Wengle [2004]).

The x-component of the internal pressure may in σ-coordinates be written as,

$$\frac{\partial \rho}{\partial x}|_z = \frac{\partial \rho}{\partial x} - \frac{\sigma}{H}\frac{\partial H}{\partial x}\frac{\partial \rho}{\partial \sigma} \ , \tag{10}$$

where ρ represents the density, H the depth, and $\sigma \equiv \frac{z-\eta}{\eta+H}$ [Berntsen, 2002]. For cases with steep topography the two terms on the right hand side may be large and of opposite signs, and may cause large errors in the estimates of the internal pressure [Berntsen, 2002]. Haney [1991] states that for the finite-difference scheme to be hydrostatic consistent, the criterion,

$$|\frac{\sigma}{\delta\sigma}\frac{\delta H}{H}| < 1 \ , \tag{11}$$

must be fulfilled. Here δH represents the horizontal change in depth between adjacent cells, and $\delta\sigma$ is the vertical grid spacing. Hence the σ-coordinate model is not suitable for simulating flow over a sharp backward facing step. We have therefore simulated flow over a rounded step, which is also more realistic in marine waters. When the depth increases, this leads to an adverse pressure gradient [Kundu and Cohen, 2004]. If the pressure gradient is large enough this can lead to separation of the flow. For flow over a rounded backward-facing step, the separation is caused by the adverse pressure gradient generated by the topography (Neumann and Wengle [2004]).

3.1 Setup

2D simulations of flow over a backward-facing step are performed, where all variables are normalized based on the step height, h, and the free-stream velocity, U_∞. The setup of a backward-facing rounded step is described in Figure 1. The rounded step starts at the point, $x = 0$, where x is the horizontal distance in meters, and is described by,

$$H(x) = \begin{cases} -100 \ , & x < 0 \ , \\ -120 + h \cdot \exp^{-\frac{x^2}{(Lh)^2}} \ , & x \geq 0 \ , \end{cases} \tag{12}$$

where L is set to 8. The grid is equidistant both in the horizontal and the vertical.

The velocity is initialized by a depth integrated velocity of 10 $\mathrm{m}^2\ \mathrm{s}^{-1}$, leading to a free flow velocity, U_∞, of 0.1 $\mathrm{m\ s}^{-1}$ before the step.

Both the left and right boundary are open. At the left boundary the velocity is described by a logarithmic layer in the bottom boundary layer, with a thickness of $\delta = 1.2h$. This is the same relation between the boundary layer and the height of the step as used in experiments by Jovic and Driver [1995], Akselvoll and Moin [1996], and Le et al. [1997]. Above the boundary layer, the velocity is set to U_∞=0.1 $\mathrm{m\ s}^{-1}$. At the right boundary the density, velocity and surface elevation are set to the average values of ρ, u, and η calculated from the mean in the 7 cells before the FRS-zone. These mean values are then used in the relaxation.

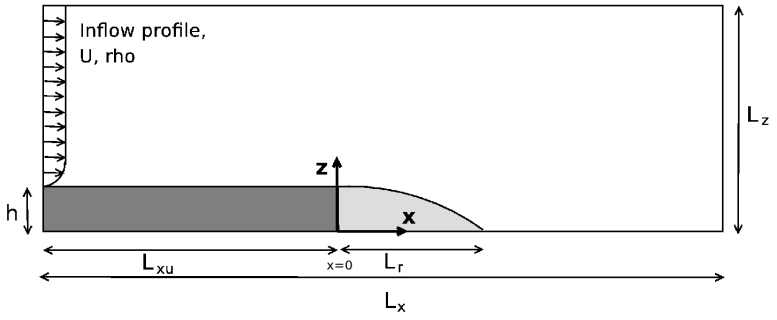

Figure 1: The setup of flow over a rounded backward-facing step. At the left boundary the velocity profile is prescribed as a logarithmic layer of thickness $\delta = 1.2h$, (as in Spalart [1988]), where h represents the height of the step. The velocity inflow in the bottom boundary layer, U_{bl}, can be described as, $U_{bl}(z') = \frac{u_*}{k}\ln z' + C$, where z' is the distance from the bottom, the friction velocity, u_* is approximated as $u_* = U_\infty/30$ and C is a constant satisfying $U_{bl}(\delta) = U_\infty$. The vertical height of the domain is set to L_z=6h= 120 meters, and the horizontal extent to $L_x = 45h$ =900 meters. The left boundary is located at $x = -10h = -200$m. The rounded backward-facing step is located at $x = 0$, and the shape of the slope is described by an exponential function (Equation (12)).

For the simulations with a horizontal resolutions of 12 to 3 meters the time step is halved as the horizontal resolution is halved. This in order to run the simulations using the same Courant numbers. For the simulations with 600x400 grid cells, we had to reduce the time step with a factor of $\frac{1}{4}$ in order to ensure numerical stability. The simulations with the highest resolution are therefore done using a lower Courant number than the coarser simulations.

The parameters used for the 20 simulations of flow over a rounded backward-facing step are presented in Table 1. In all simulations the length of the domain is 900 meters, and the height of the step, h, is 20 meters.

3.2 Results

In Table 2 the separation point and mean reattachment lengths are presented. The separation point and reattachment lengths are calculated based on the mean horizontal velocities between 12 and 24 hours. The reattachment point and the separation point is defined as the point where the average velocity between 12 and 24 hours is zero, i.e. where the probability of negative velocities equals the probability of positive velocities [Kasagi and Matsunaga, 1995]. These points are defined as the boundaries of the reattachment zone.

Figure 2 shows the horizontal bottom velocities using a resolution of 300x200 grid cells. There are no negative velocities using Reynolds numbers of $2{\cdot}10^3$ (Simulation B7, Figure 2 a)), as can also be seen from Table 2. For these cases the flow is stationary. Using Reynolds numbers of $2{\cdot}10^5$ (Simulation B15, Figure 2 b)), negative velocities occur at the slope after a 6 hour long spin up period. The separation point is fluctuating to a much smaller extent than the reattachment point. Also notice the "dead water region" downstream the separation point with very low horizontal velocities. For Reynolds numbers less or equal to $2{\cdot}10^3$ the flow is stationary and there is no separation of the flow. In other words no eddies are generated behind the step. For higher Reynolds numbers the flow separates on the rounded slope, additionally the flow varies in time. Eddies are generated downstream the step. In time, eddies are released from the reattachment zone and propagates downstream with a

Simulation	Number of grid cells	Δx [m]	Δt [s]	K_M/K_H [m^2s^{-1}]	Re [-]
B1	75x50	12	4	10^2	$2{\cdot}10^2$
B2	150x100	6	2	10^2	$2{\cdot}10^2$
B3	300x200	3	1	10^2	$2{\cdot}10^2$
B4	600x400	1.5	0.25	10^2	$2{\cdot}10^2$
B5	75x50	12	4	10^3	$2{\cdot}10^3$
B6	150x100	6	2	10^3	$2{\cdot}10^3$
B7	300x200	3	1	10^3	$2{\cdot}10^3$
B8	600x400	1.5	0.25	10^3	$2{\cdot}10^3$
B9	75x50	12	4	10^4	$2{\cdot}10^4$
B10	150x100	6	2	10^4	$2{\cdot}10^4$
B11	300x200	3	1	10^4	$2{\cdot}10^4$
B12	600x400	1.5	0.25	10^4	$2{\cdot}10^4$
B13	75x50	12	4	10^5	$2{\cdot}10^5$
B14	150x100	6	2	10^5	$2{\cdot}10^5$
B15	300x200	3	1	10^5	$2{\cdot}10^5$
B16	600x400	1.5	0.25	10^5	$2{\cdot}10^5$
B17	75x50	12	4	10^6	$2{\cdot}10^6$
B18	150x100	6	2	10^6	$2{\cdot}10^6$
B19	300x200	3	1	10^6	$2{\cdot}10^6$
B20	600x400	1.5	0.25	10^6	$2{\cdot}10^6$

Table 1: The number of grid cells, the horizontal resolution, the time step, the vertical eddy viscosity and diffusivity, and the Reynolds numbers, $Re = \frac{U_\infty h}{\nu}$, used in the simulations of flow over a rounded backward-facing step.

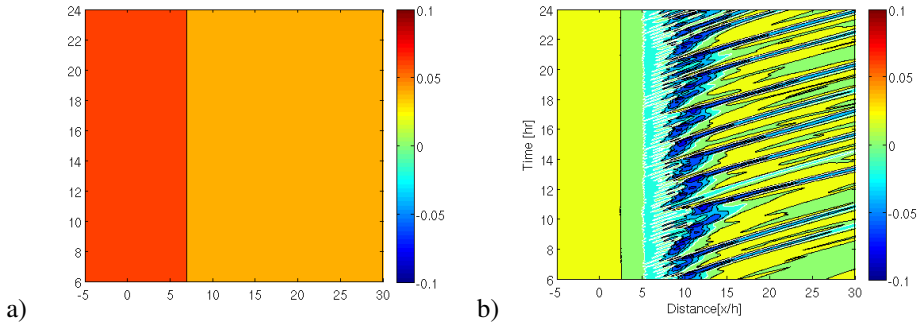

Figure 2: The bottom velocities using a Reynolds number of a) Re=$2{\cdot}10^3$ (B7) and b) Re=$2{\cdot}10^4$ (B15).

Re		$2{\cdot}10^2$	$2{\cdot}10^3$	$2{\cdot}10^4$	$2{\cdot}10^5$	$2{\cdot}10^6$
Separation	150x100	-	-	5.90	4.10	3.80
X_s/h	300x200	-	-	5.30	1.40	0.80
	600x400			5.83	2.07	5.75*
Reattachment	150x100	-	-	21.2	17.6	17.0
X_r/h	300x200	-	-	15.4	8.15	13.0
	600x400	-	-	18.0	11.0	10.3/18.4*

Table 2: The reattachment point and the separation point for flow over a backward-facing step, L=8. *two clockwise eddies occur.

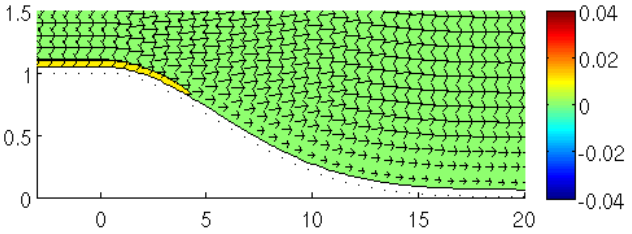

a)

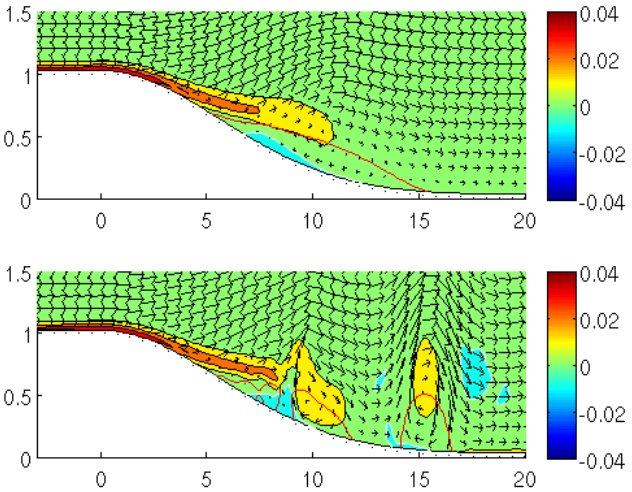

b)

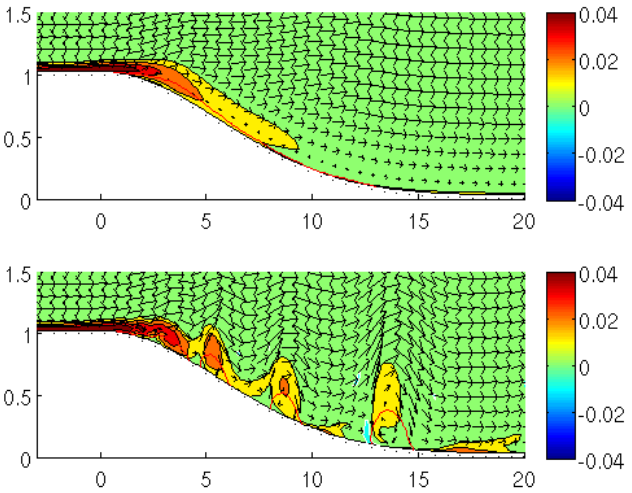

c)

Figure 3: The mean vorticity and the velocity arrows from 12 to 24 hours and a snapshot of the vorticity and the velocity arrows at 24 hours for Simulation a) B7, b) B11, and c) B19. The red line gives the positions where $U = 0$ m s^{-1}.

velocity of approximately 3 cm s^{-1}(Simulation B15, Figure 2b)).

Figure 3 shows the mean vorticity and velocity arrows from 12 to 24 hours and a snapshot of the vorticity and the velocity arrows at 24 hours using a resolution of 300x200 grid cells (Simulation B7). The mean profile and the snapshot of the horizontal vorticity coincide for the simulations with Reynolds numbers of $2{\cdot}10^3$, showing that the flow is stationary. As the viscosities are reduced the eddies evolve further up the slope, leading to a shift upstream in the average reattachment zone.

4 Flow over a depression

Though pockmarks and plough marks usually have a horizontal dimension of 50 meters, we have chosen to study a wider depression to reduce the effect on the reattachment zone from the forward facing step at the downstream side.

4.1 Setup

The total horizontal extent of the domain is set to 1500 meters. The depression is located in the middle of the domain and has a 500 meter long flat bottom. At the ends, the slopes are described by an exponential function,

$$H(x) = \begin{cases} -100\ , & x < 0\ , \\ -(100+h) + h \cdot \exp^{-\frac{x^2}{(Lh)^2}}\ , & x \geq 0, x \leq \chi\ , \\ -(100+h)\ , & x > \chi,\ x < \chi + 500\ , \\ -(100+h) + h \cdot \exp^{-\frac{(500+2\chi-x)^2}{(Lh)^2}}\ , & x \geq \chi + 500,\ x \leq 500 + 2\chi\ , \\ -100\ , & x > 500 + 2\chi \end{cases} \tag{13}$$

Simulations are performed with three different depths, h, of the depression, two different slopes χ and three different ambient velocities U_∞. All simulations are done using horizontal eddy viscosities of 10^{-2} m^2 s^{-1}. We have chosen to use constant vertical eddy viscosities and diffusivities of 10^{-4} m^2 s^{-1} for a horizontal resolution of 3 meters. This choice is based on a study of flow over a sharp backward facing step using the MITgcm (Massachusetts Institute of Technology general circulation model) which is compared with theory, and a convergence study of flow over a rounded step using the MITgcm and BOM [Rygg et al.].

In all simulations we have initialized the model with a depth integrated velocity. The horizontal resolution is 3 meters and we have used an equidistant layering in the vertical where the total depth has been discretized with 100 layers. The minimum depth in the domain is 100 meters. All boundaries are open and are defined as for the flow over a backward-facing round step, but the thickness of the logarithmic layer is set fixed to $\delta = 1.2 \cdot 20$ meters for all simulations, leading to the same inflow boundary condition for the horizontal velocity for all simulations. The simulations have been run for 24 hours.

4.2 Results

Table 4.2 shows the separation point and the reattachment point based on the average velocity profile from 12-24 hours. For the cases with the same depth integrated velocity the depth of the separation point can be found at approximately the same depth (see column 6 in Table 4.2). Hence as h increases, the thickness of the boundary layer downstream the separation point also increases, leading to larger eddies and more intense eddies for the scenarios with a deep depression (20 meters depth) compared to the less deep depression (10 meters depth). For the cases with $h = 10$ meter and an ambient velocity of 5 cm s^{-1}, no separation occur.

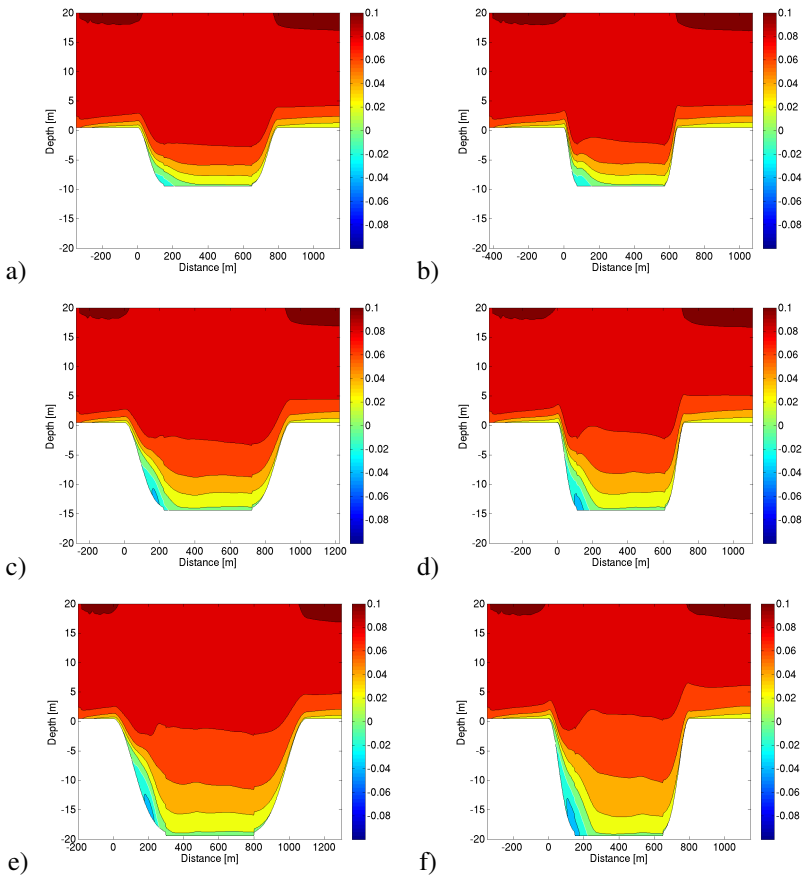

Figure 4: The mean horizontal velocity from 12-24h for Simulation a) D4, b) D13, c) D5, d) D14, e) D6, and f) D15.

For steeper slopes, the variation in H_s (the depth of the separation point) increases, most likely due to the growth in the internal pressure error. Both the average separation point and the average reattachment points have the tendency to move upstream with increasing Reynolds numbers.

Figure 4 shows the horizontal velocity profiles from 12-24 hours, and Figure 5 a snapshot of the horizontal velocity at 24 hours after simulation start for Simulation D4-D6 and D13-D15. The height of the eddies downstream the separation point increases with increasing depth of the depression, and the intensity of the eddies also increases (can be seen by the increasing negative horizontal velocities with depth). The eddies are also higher and more intense for the steep slope case compared to the simulations with gentler slopes (the left figures in Figure 5).

Figure 7 shows the paths of eight tracers released at x= -64 m and at different depths, z_0, released at 6 hours simulation time. This simulation is done using the serial 2D version of BOM. The particles tend to avoid the recirculation zone, and the eddies downstream the separation point can be observed. The red stars show the average separation and reattachment point from 6 to 12 hours, and the black diamonds where particles have been taken out of the simulation.

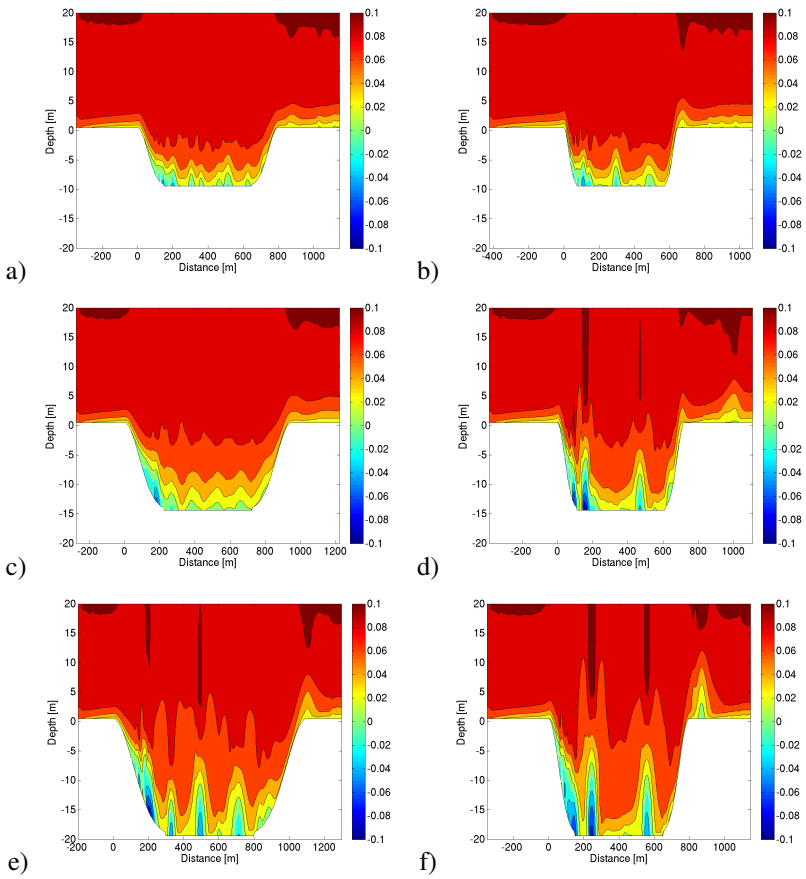

Figure 5: A snapshot of the horizontal velocity at 24h for Simulation a) D4, b) D13, c) D5, d) D14, e) D6, and f) D15.

5 Discussion

5.1 Backward-facing rounded step

In 2004 Bao and Dallmann [2004] did laboratory experiments on flow over a rounded step in a water tunnel using particle image velocimetery. According to this paper, the laminar separation first occurred for Reynolds numbers of 2700, before this point there was no separation of the flow. This observation corresponds with our simulations with no separation of the flow for Reynolds numbers lower than or equal to 2000.

In all the experiments by Bao and Dallmann [2004] the separated flow region was characterized by several discrete vortex structures that propagated downstream. As the vortexes moved downstream new eddies were generated next to the separation point, also in correspondence with our model results.

Bao and Dallmann [2004] also registered that the separation point and the angle of the separation point were constant in time in spite of the unsteady eddies generated right downstream the separation point. The near constant position of the separation point is also observed through our simulations.

The simulations show some variation in both separation point and reattachment point as the resolution and eddy viscosities are reduced. It is no clear convergence of the mean reattachment point, but due to the time dependence of the flow it is difficult to compare different works and different simulations.

According to Barton [1995] neutral particles for flow over a backward-facing step tend

	h [m]	L -	χ [m]	U_∞ [m s^{-1}]	h/χ -	X_s [m]	H_s [m]	X_r [m]	H_r [m]
D1	10	8	150	0.05	0.067	-	-	-	-
D2	15	8	225	0.05	0.067	192	-13.9	309	-15.0
D3	20	8	300	0.05	0.067	159	-12.6	549	-20.0
D4	10	8	150	0.1	0.067	99.0	-7.9	207	-10.0
D5	15	8	225	0.1	0.067	96.0	-7.20	249	-15.0
D6	20	8	300	0.1	0.067	105	-7.11	261	-18.6
D7	10	8	150	0.2	0.067	54.0	-3.77	159	-10.0
D8	15	8	225	0.2	0.067	57.0	-3.13	192	-13.9
D9	20	8	300	0.2	0.067	69.0	-3.48	207	-16.3
D10	10.0	4	75	0.05	0.13	-	-	-	-
D11	15	4	112.5	0.05	0.13	69.0	-11.4	258	-15.0
D12	20	4	150	0.05	0.13	66.0	-10.1	291	-20.0
D13	10	4	75	0.1	0.13	45.0	-7.34	156	-10.0
D14	15	4	112.5	0.1	0.13	36.0	-5.06	180	-15.0
D15	20	4	150	0.1	0.13	39.0	-4.42	222	-20.0
D16	10	4	75	0.2	0.13	21.0	-2.61	120	-10.0
D17	15	4	112.5	0.2	0.13	18.0	-1.65	138	-15.0
D18	20	4	150	0.2	0.13	8.0	-1.10	144	-19.3

Table 3: The separation and the reattachment points, calculated from the mean bottom velocities between 12-24 hours, h represents the height of the depression, L a parameter determening the length of the slope (Equation (13)), χ the length of the slope, U_∞ the free stream velocity before the depression, h/χ the steepness of the slope, X_s the horizontal position of the separation point, H_s the depth of the separation point, X_r the horizontal position of the average reattachment length from 12-24 hours, and H_r the depth of the reattachment point.

to follow the streamlines. Fessler and Eaton [1999] observed that for a sharp backward-facing step, few particles were found within the recirculation zone. If this result also is relevant for a backward rounded step, the recirculation zone will not be a suitable location for living corals.

5.2 Flow over a depression

For flow over a wide depression, approximately the same separation points and reattachment points can be observed as for flow over a backward-facing step for the same Reynolds numbers. The resemblance between these two setups are due to the wideness of the depression. If the depression were shorter this would affect the flow at the upstream slope of the depression.

For the same slope, and varying ambient velocities, the separation point can be observed at approximately the same depth, the larger height difference between the bottom of the depression and the separation point leads to fiercer eddies for deeper depressions.

Frederiksen et al. [1992] observed a correlation between the occurrence of Lophelia Pertusa and breaking of internal waves at the shelf of the Faeroe Islands. He suggested that there are two ways the breaking waves could increase the food transport to the corals, by "inducing resuspension of organic matter from the sea-bottom leading to increased food supply downslope from the mixing region", or by an "increased vertical nutrient nutrient flux through the thermocline" [Frederiksen et al., 1992]. The eddies generated downstream the separation point lead to an increase in the vertical transport. Due to the vortex downstream the separation point based on the mean profile and the low velocities in this regime the reattachment zone is most likely a less suitable location for corals.

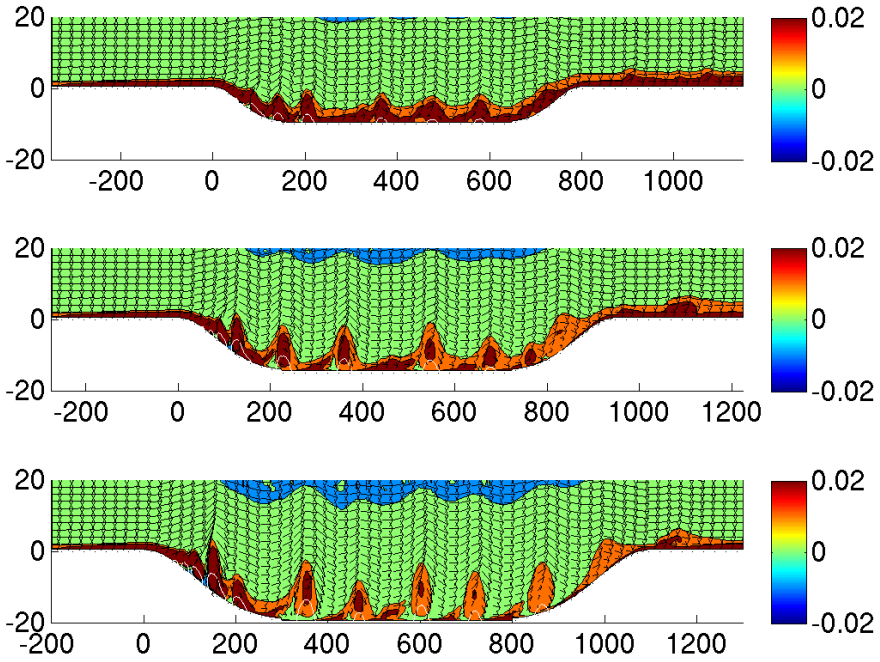

Figure 6: The vorticity at 24h, the white line shows where the horizontal velocity, U, equals zero for Simulation D4-D6.

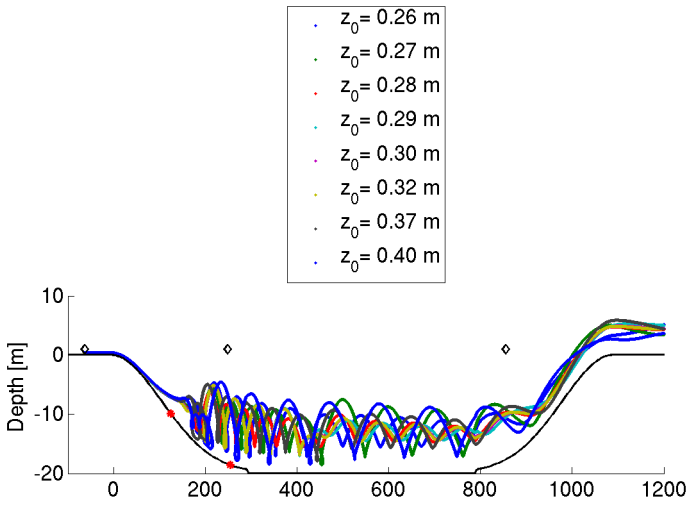

Figure 7: The paths of 8 particles released after 6 hours at x =-64 meters at z_0 meter above the bottom. The diamonds represents where passive tracers have been taken out of the simulations, and the red stars represents the mean separation point and the mean reattachment point from 6 to 24 hours simulation time.

6 Summary

Simulations of flow over a backward-facing step and flow over a depression have been done using the 2D version of Bergen Ocean Model. The model results correspond well with published observational results. Hence this study gives a basis for verification of the model for application to the flow over a pockmark or plough mark in the future. Future studies will also include pockmarks and plough marks of realistic sizes.

Acknowledgment

This research has received support from The Research Council of Norway through NFR 146526/420: Cordino.

References

K. Akselvoll and P. Moin. Large eddy simulatin of turbulent confined coannular jets and turbulent flow over a backward facing step. *Journal of Fluid Dynamics*, (315):387–411, 1996. 3.1

F. Bao and U. C. Dallmann. Some physical aspects of separation bubble on a rounded backward-facing step. *Aerospace Science and Technology*, 8:83–91, 2004. 5.1

I. E. Barton. Computation of particle tracks over a backward-facing step. *Journal of Aerosol Science*, 26(6):887–901, 1995. 5.1

J. Berntsen. USERS GUIDE for a modesplit σ-coordinate numerical ocean model. Technical Report 4.1, University of Bergen, Johs. Bruns gt. 12, N-5008 BERGEN, 2004. 2, 2

J. Berntsen. Internal pressure errors in sigma-coordinate ocean models. *Journal of atmospheric and oceanic technology*, 19:1403–1414, 2002. 3

J. Berntsen, J. Xing, and G. Alendal. Assessment of non-hydrostatic ocean models using laboratory scale problems. *Continental Shelf Research*, (26):1433–1447, 2006. 2

J. R. Fessler and J. K. Eaton. Turbulence modifiaction by particles in a backward-facing flow. *Journal of Fluid Mechanics*, 394:97–117, 1999. 5.1

J. H. Fosså, P. B. Mortensen, and D. M. Furevik. The deep-water coral Lophelia pertusa in Norwegian waters: distribution and fishery impacts. *Hydrobiologica*, 2002. 1

R. Frederiksen, A. Jensen, and H. Westerberg. The distribution of the scleractinian coral Lophelia pertusa around the Faroe Islands and the relation to internal mixing. *Sarsia*, 77:157–171, 1992. 5.2

A. Freiwald, J. B. Wilson, and R. Henrich. Grounding pleistocene icebergs shape recent deep-water coral reefs. *Sedimentary Geology*, 125:1–8, 1999. 1

A. Freiwald, J. H. Fosså, A. Grehan, T. Koslow, and J. M. Roberts. Cold-water corals reefs. out of sight no longer out of mind. *UNEP-WCMC, Cambridge, UK*, 2004. 1

R. L. Haney. On the pressure gradient force over steep topography in sigma coordinate ocean models. *Journal of Physical Oceanography*, 1991. 3

M. Hovland and A. G. Judd. *Seabed pockmarks and seepages: impact on geology, biology and the marine environment*. London: Graham & Trotman, 1988. 1

S Jovic and D Driver. Reynolds number effect on the skin friction in separated flows behind a backward-facing step. *Experimental Fluids*, (18):464–467, 1995. 3.1

N. Kasagi and A. Matsunaga. Three-dimensional particle-tracking velocimetry measurement of turbulence statistics and energy budget in a backward-facing step flow. *International journal of Heat and Fluid Flow*, 16:477–485, 1995. 3.2

P. K. Kundu and I. M. Cohen. *Fluid mechanics*. Elsevier Academic Press, 3rd edition, 2004. ISBN 0-12-178253-0. 3

H. Le, P. Moin, and J. Kim. Direct numerical simulation of turbulent flow over a backward-facing step. *Journal of Fluid Dynamics*, (330):349–373, 1997. 3.1

R. Lien. Pløyemerker etter isfjell på norsk kontinentalsokkel (Iceberg scouring on the Norwegian continental shelf). *IKU Publication*, 1983. 1

B. Lindberg, C. Berndt, and J. Mienert. The Fugløy reef at 70^oN; acoustic signature, geologic, geommorphologic and oceanographic setting. *International Journal of Earth Science*, 96:201–213, 2007. 1

J. Marshall, A. Adcroft C. Hill, L. Perelman, and C. Heisey. A finite-volume, incompressible Navier Stokes model for studies of the ocean on parallel computer. *Journal of geophysical research*, 102(C3):5753–5766, 1997a. 2

J. Marshall, C. Hill, L. Perelman, and A. Adcroft. Hydrostatic, quasi–hydrostatic, and nonhydrostatic ocean modeling. *J. Geophys. Res.*, 102(C3):5733–5752, 1997b. 2

E. A. Martinsen and H. Engedahl. Implementation and testing of a lateral boundary scheme as an open boundary condition in a barotropic ocean model. *Coastal Engineering*, (11): 603–627, 1987. 2.2, 2.2

P. B. Mortensen, M. T. Hovland, J. H. Fosså, and D. M. Furevik. Distribution, abundance and size of lophelia pertusa coral reefs in mid-Norway in relation to seabed characteristics. *Journal of Marine Biology Association*, 81:581–597, 2001. 1

J. Neumann and H. Wengle. Coherent structures in controlled separated flow over sharp-edged and rounded steps. *Journal of Turbulence*, 5(022):1–24, 2004. 3, 3

K. Rygg, G. Alendal, and P. M. Haugan. Flow over a backward-facing step, a convergence study comparing a z-coordinate model and a σ-coordinate model. In preparation. 4.1

P. R. Spalart. Direct simulation of a turbulent boundary layer up to Re_θ=1410. *Journal of Fluid Mechanics*, 187:61–98, 1988. 1

Ø. Thiem, J. Berntsen, K. Selvikvåg, and J.H. Fosså. Numerical study of particle encounters with an idealized coral reef with focus on grid resolutions and viscosities. Technical report, UNIFOB AS, 2008. 1